Proceedings of the
International Conference on Mechanical Engineering and Renewable Energy 2015
(ICMERE2015) 26 – 29 November, 2015, Chittagong, Bangladesh

ICMERE2015-PI-058

PERFORMANCE OF NANOFLUID IN FREE CONVECTIVE HEAT TRANSFER INSIDE A CAVITY WITH NON-ISOTHERMAL BOUNDARY CONDITIONS

Salma Parvin[1,*], Raju Chowdhury[2], M.A.H Khan[3] and M.A. Alim[4]

[1 – 4]Department of Mathematics, Bangladesh University of Engineering & Technology, Dhaka-1000, Bangladesh
[2]Department of Natural Science, Stamford University Bangladesh, Dhaka-1209, Bangladesh.
[1,*]salpar@math.buet.ac.bd, [2]raju_chy_23@yahoo.com, [3]mahkhan@math.buet.ac.bd, [4]maalim@math.buet.ac.bd

Abstract*-The free convective flow and heat transfer characteristics of nanofluid inside a prismatic enclosure with non-uniform temperature distribution maintained at the bottom wall is analyzed numerically. The water based nanofluid with alumina nanoparticle is used as the operational fluid through the enclosure. The governing partial differential equations with proper boundary conditions are solved by Finite Element Method using Galerkin's weighted residual scheme. Calculations are performed for different solid volume fraction of nanoparticles $0 \le \chi \le 0.1$ with Rayleigh number 10^5. An enhancement in heat transfer rate is observed with the increase of nanoparticles volume fraction.*

Keywords: Natural Convection; finite element method; Nanofluid; Solid Volume Fraction; Prismatic enclosure

1. INTRODUCTION

Many engineering applications of natural convection in encloseres including geophysics, geothermal reservoirs, insulation of building, heat exchanger design, building structure etc. motivate many researchers to perform numerical simulation to investigate the flow pattern, temperature distribution, and heat flow. The low thermal conductivity of conventional heat transfer fluids, commonly water, has restricted designers. Fluids containing nanosized solid particles offer a possible solution to conquest this problem. The nanofluid has greater effective thermal conductivity than pure base fluid. Most of the available literature on this topic concerns regular geometries such as rectangular or square enclosures, while actual applications demand the consideration of irregular shapes. Literature reviews on natural convection inside triangular, trapezoidal and rhombic enclosures are available in [1-5]. In view of various applications of thermal processes, a comprehensive understanding of heat transfer and flow circulations within prismatic cavities is very much essential for industrial development. Current work attempts to analyze heat transfer and energy distributions using heatline concept inside a nanofluid filled prisamtic cavity.

The heat recovery system or true path of convective heat transfer can be visualized by 'heatline' method. Kimura and Bejan [6] and Bejan [7] first introduced the concept of heatline. Heatlines represent heatflux lines which represent the trajectory of heat flow in the system and they are normal to the isotherms for conductive heat transfer. Various applications using heatlines were studied by Bello-Ochende [8], Costa [9-11], Mukhopadhyay et al. [12,13] and Deng and Tang [14]. Dalal and Das [15] have used heatline method for the visualization of flow in a complicated cavity. Recently, Yaseen [16] has studied and analyzed numerically the steady natural convection flow in a prismatic enclosure with strip heater on bottom wall. For this enclosure, top inclined walls are considered at low temperature, two vertical walls were adiabatic and strip heater was at constant high temperature mounted on the bottom enclosure while the reminder bottom wall was kept at low temperature. Recently Ahmed et.al [17] performed numerical analysis for natural convection flows within prismatic enclosures based on heatline approach.

Heat transfer in cavities filled with nanofluid is the research interest of many researchers. Parvin et al. [18] studied the natural convection heat transfer in an enclosure with a heated body filled with nanofluid. Nasrin and Parvin [19] investigated numerically the buoyancy-driven flow and heat transfer in a trapezoidal cavity filled with water–Cu nanofluid. In their work, a correlation is developed graphically for the average Nusselt number as a function of the Prandtl number as well as the cavity aspect ratio. Abu- Nada and Chamkha [20] performed a numerical study of natural convection heat transfer in a differentially heated enclosure filled with CuO-EG-Water nanofluid. The results were compared with Brinkman model and MG models for nanofluid viscosity and thermal conductivity. Either enhancement or decline was reported for the average Nusselt number as the volume fraction of nanoparticles increased. Heat Transfer and Entropy Generation in an Odd-shaped Cavity filled with Nanofluid is analyzed by Parvin and Chamkha [21]. It must be noticed that, adding nanoparticles into the base fluid does not always increase its thermal conductivity [22]. Teja et al. [24] have reported that the thermal conductivity of 2 nm titania nanoparticles is smaller than the thermal conductivity of the base fluid at the same temperature. Parvin et al. [23] numerically investigated the natural convection heat transfer from a heated cylinder contained in a square enclosure filled with water–Cu nanofluid. Their results indicated that heat transfer augmentation is possible using highly viscous nanofluid.

From the above discussion, the literature contains many investigations into the heat transfer performance of natural convection of nanofluid in regular shaped cavities. However, a comprehensive analysis on heat flow during natural convection of nanofluid in irregular enclosure with the heatline approach is yet to appear in the literature. Accordingly, the present study performs a numerical investigation into the natural convection heat flow within a prism shaped cavity containing nanofluid with non isothermal bottom wall. The simulations focus specifically on the effects of the different volume fraction of nanofluid on the streamlines, isotherm distribution, heatlines and average Nusselt number. Average temperature and velocity are also presented.

2. MATHEMATICAL FORMULATION

2.1 Momentum and energy formulation

The physical domain is shown in Fig. 1. The fluid properties are assumed to be constant except the density variation which is determined according to the Boussinesq approximation. Under these assumptions, the governing equations for steady two dimensional laminar incompressible flows can be written in dimensionless form as:

$$\frac{\partial U}{\partial X}+\frac{\partial V}{\partial Y}=0 \qquad (1)$$

$$U\frac{\partial U}{\partial X}+V\frac{\partial U}{\partial Y} = -\frac{\rho_f}{\rho_{nf}}\frac{\partial P}{\partial X}+Pr\frac{\nu_{nf}}{\nu_f}\left(\frac{\partial^2 U}{\partial X^2}+\frac{\partial^2 U}{\partial Y^2}\right) \qquad (2)$$

$$U\frac{\partial V}{\partial X}+V\frac{\partial V}{\partial Y} = -\frac{\rho_f}{\rho_{nf}}\frac{\partial P}{\partial Y}+Pr\frac{\nu_{nf}}{\nu_f}\left(\frac{\partial^2 V}{\partial X^2}+\frac{\partial^2 V}{\partial Y^2}\right) + Ra\,Pr\frac{(1-\chi)\rho_f\beta_f+\chi\rho_s\beta_s}{\rho_{nf}\beta_f}\,\theta \qquad (3)$$

$$U\frac{\partial \theta}{\partial X}+V\frac{\partial \theta}{\partial Y}=\frac{\alpha_{nf}}{\alpha_f}\left(\frac{\partial^2 \theta}{\partial X^2}+\frac{\partial^2 \theta}{\partial Y^2}\right) \qquad (4)$$

where, $\rho_{nf}=(1-\chi)\rho_f+\chi\rho_s$ is the density,

$(\rho C_p)_{nf}=(1-\chi)(\rho C_p)_f+\chi(\rho C_p)_s$ is the heat capacitance, $\beta_{nf}=(1-\chi)\beta_f+\chi\beta_s$ is the thermal expansion coefficient, $\alpha_{nf}=k_{nf}/(\rho C_p)_{nf}$ is the thermal diffusivity, $\mu_{nf}=\mu_f(1-\chi)^{-2.5}$ is dynamic viscosity and

$k_{nf}=k_f\dfrac{k_s+2k_f-2\chi(k_f-k_s)}{k_s+2k_f+\chi(k_f-k_s)}$ is the thermal conductivity of the nanofluid and

$$X=\frac{x}{L},\ Y=\frac{y}{L},\ U=\frac{uL}{\alpha},\ V=\frac{vL}{\alpha},\ \theta=\frac{T-T_c}{T_h-T_c},$$
$$P=\frac{pL^2}{\rho\alpha^2},\ \Pr=\frac{\nu}{\alpha},\ Ra=\frac{g\beta(T_h-T_c)L^3\Pr}{\nu^2} \qquad (5)$$

The boundary conditions can be summarized by the following equations:

- At the bottom wall: $U=0, V=0, \theta=\sin(\pi L)$
- For the side walls: $U=0, V=0, \dfrac{\partial\theta}{\partial X}=0$
- For the inclined walls: $U=0, V=0, \theta=0$

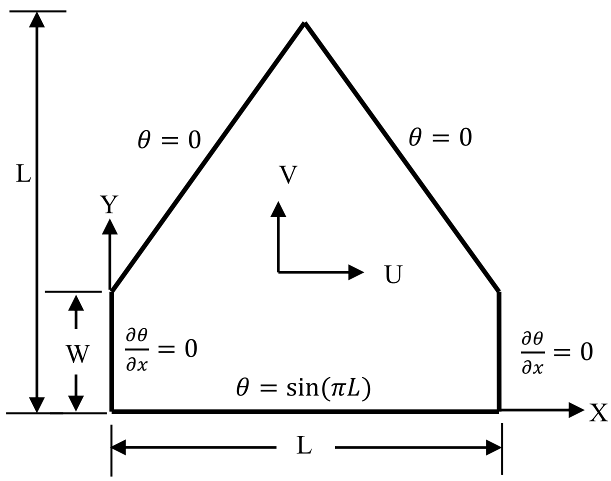

Fig.1: Schematic diagram of the physical system

2.2 Streamfunction and heatfunction

The relationships between streamfunction ψ and velocity components *U*, *V* for two-dimensional flows are

$$U=\frac{\partial\psi}{\partial Y}\ \text{and}\ V=-\frac{\partial\psi}{\partial X} \qquad (6)$$

which give a single equation

$$\frac{\partial^2\psi}{\partial X^2}+\frac{\partial^2\psi}{\partial Y^2}=\frac{\partial U}{\partial Y}-\frac{\partial V}{\partial X} \qquad (7)$$

The no-slip condition is valid at all boundaries as there is no cross-flow. Hence $\psi=0$ is used for boundaries. The heat flow within the enclosure is displayed using the heatfunction *Π* obtained from conductive heat fluxes $\left(-\frac{\partial\theta}{\partial X},-\frac{\partial\theta}{\partial Y}\right)$ as well as convective heat fluxes (*Uθ*, *Vθ*). The heatfunction satisfies the steady energy balance equation (Eq. (4)) such that

$$\frac{\partial\Pi}{\partial Y}=U\theta-\frac{\partial\theta}{\partial X}\ \text{and}\ -\frac{\partial\Pi}{\partial X}=V\theta-\frac{\partial\theta}{\partial Y} \qquad (8)$$

which yield a single equation

$$\frac{\partial^2\Pi}{\partial X^2}+\frac{\partial^2\Pi}{\partial Y^2}=\frac{\partial}{\partial Y}(U\theta)-\frac{\partial}{\partial X}(V\theta) \qquad (9)$$

2.3 Average Nusselt number

The average Nusselt number, average temperature and average velocity may be expressed as

$$Nu=-\frac{1}{S}\int_0^S\left(\frac{k_{nf}}{k_f}\right)\frac{\partial\theta}{\partial N}\,dN$$

$$\theta_{av}=\int\theta\,d\bar{V}/\bar{V} \text{ and } V_{av}=\int V\,d\bar{V}/\bar{V}$$

where S is the non-dimensional length of the surface and $\bar{V}$ is the volume to be accounted.

3. NUMERICAL IMPLEMENTATION

The Galerkin finite element method is used to solve the non-dimensional governing equations along with boundary conditions for the considered problem. The equation of continuity has been used as a constraint due to mass conservation and this restriction may be used to find the pressure distribution. The finite element method of Reddy [24] is used to solve the Eqns. (6) - (9) where the pressure P is eliminated by a constraint. The continuity equation is automatically fulfilled for large values of this penalty constraint. Then the velocity components (U, V) and temperature (θ) are expanded using a basis set. The Galerkin finite element technique yields the subsequent nonlinear residual equations. The non-linear residual equations are solved using Newton–Raphson method to determine the coefficients of the expansions. The convergence of solutions is assumed when the relative error for each variable between consecutive iterations is recorded below the convergence criterion ε such that $\left|\psi^{n+1}-\psi^{n}\right|\le 10^{-4}$, where n is the number of iteration and ψ is a function of U, V and θ.

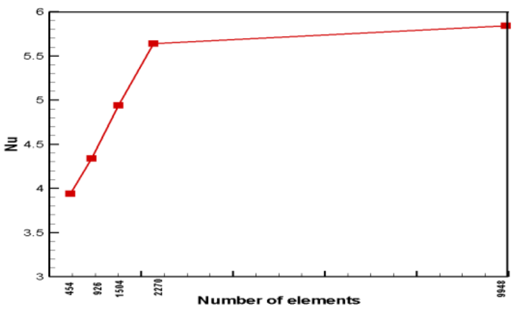

Fig.2: Grid independent test

3.1 Grid Independent Test

An extensive mesh testing procedure is conducted to guarantee a grid-independent solution for Ra = 10^5 and Pr = 6.2, χ = 0 in a prismatic enclosure. Five different non-uniform grid systems with the following number of elements within the resolution field: 454, 926, 1504, 2270 and 9948 are exami8ned. The numerical scheme is carried out for highly precise key in the average Nusselt (Nu) number to understand the grid fineness as shown in Fig. 2. The scale of the average Nusselt numbers for 2270 elements shows a little difference with the results obtained for the other elements. Hence, considering the non-uniform grid system of 2270 elements is preferred for the computation.

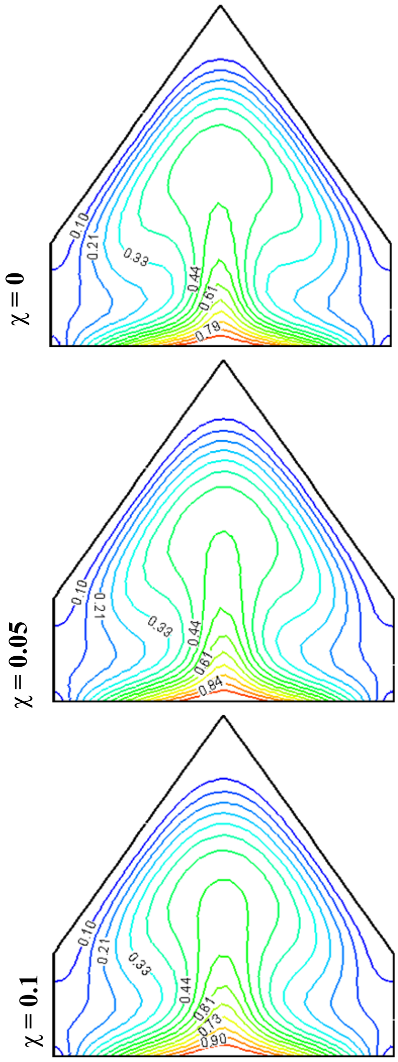

Fig.3. Effect of χ on Isothems

4. RESULTS AND DISCUSSION

The numerical computation has been carried out through the finite element method to analyze natural convection within a nanofluid filled prismatic enclosure based on heatline concept. Results of isotherms, streamlines and heatlines for various values of nanoparticle volume fraction χ (=0, 0.05, 0.1) with Rayleigh number Ra = 10^5 and Prandtl number Pr = 6.2 in the prismatic enclosure are displayed. In addition, the values of average Nusselt number at the top inclined walls and the bottom wall as well as average temperature and average velocitiy in the cavity have been calculated for the mentioned parameter.

4.1 Effect on Isotherms

The influence of particle volume fraction χ on isotherms for the present configuration has been demonstrated in Fig. 3. The pattern of isotherms are smooth and are symmetric to the central vertical line for all the considered values of χ. A thermal plume rises from the middle of the bottom wall because of sinusoidal boundary temperature. At $\chi = 0$, that is in the case of base fluid, the higher temperature lines remain near the hot bottom wall. These lines move toward the cold top inclined walls due to the increasing values of χ. This happens due to the presence of nanoparticle in the fluid and buoyancy effect which causes higher temperature gradient and thus the isothermal lines move from hot walls to the cold wall.

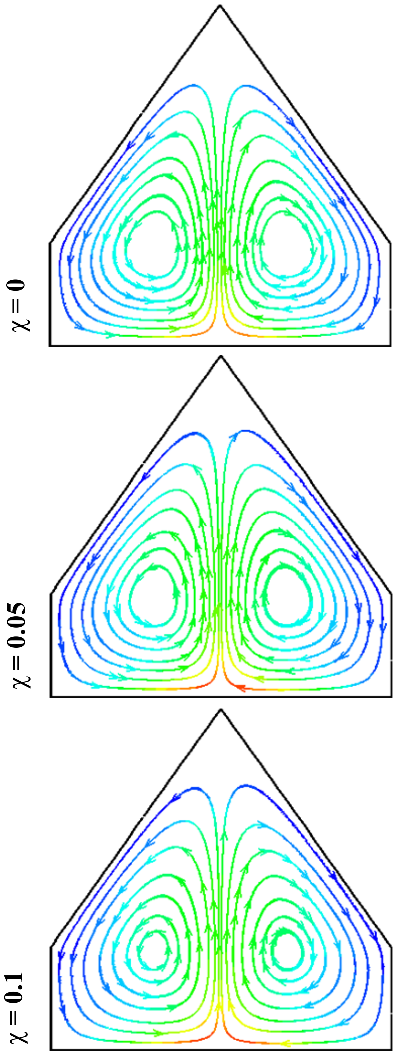

Fig.4. Effect of χ on streamlines

4.2 Effect on Streamlines

Streamlines corresponding to different nanofluid solid volume fraction χ are shown in Fig. 4. It is seen from the figure that the trend of streamlines are similar for all cases. There are two symmetric circulation cells formed inside the enclosure. With the increasing value of the χ the streamlines are less dense near the central vertical line. It is noteworthy to mention that the central core of the circulatory cell is reduded in size for higher nanoparticle concentration. Higher flow intensity is seen for the base fluid.

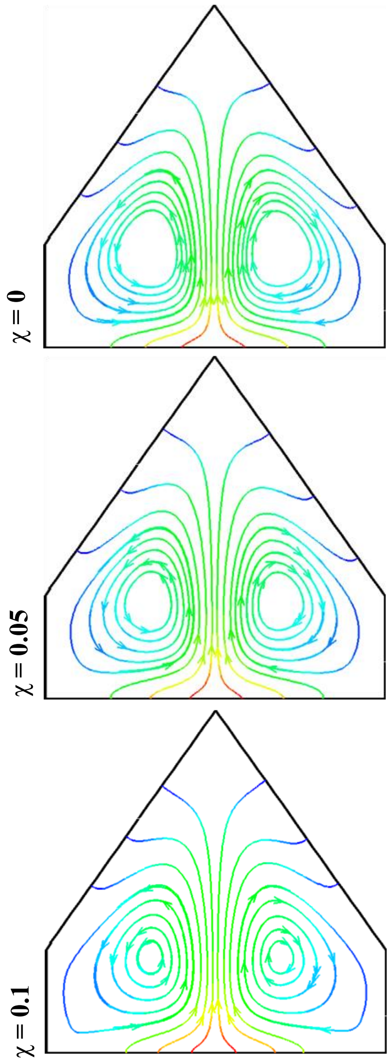

Fig.5. Effect of χ on heatlines

4.3 Effect on Heatlines

The heatlines are constructed based on the thermal boundary conditions. As seen from the Fig. 5, the heatlines are similar to streamlines at the core signifying convective heat flow and a large amount of heat flow occurs from the middle portion of the bottom wall as seen from dense heatlines. The two heat circulations in the system are observed and a very intense heat flow occurs across the middle of the cavity represented by dense heatline for pure water. It is interesting to observe that heat transport in a large regime at the core is due to convection. The large regime of convection is due to the large amount of heat transport from the bottom wall associated with large intensity of circulations. As the value of χ increases the convective heat transport has been suppressed.

4.4 Average Nusselt number

Fig. 6 shows the distribution of the average Nusselt number of the top inclined walls and bottom wall versus the solid volume fraction of nanofluid. General observation is that the average Nusselt number increases with nanoparticle concentration and it is utilized to represent the overall heat transfer rate within the domain. Similar trend of heat transfer is seen for both the walls. That is adding nanoparticles increases the thermal conductivity which leads to enhanced heat transfer.

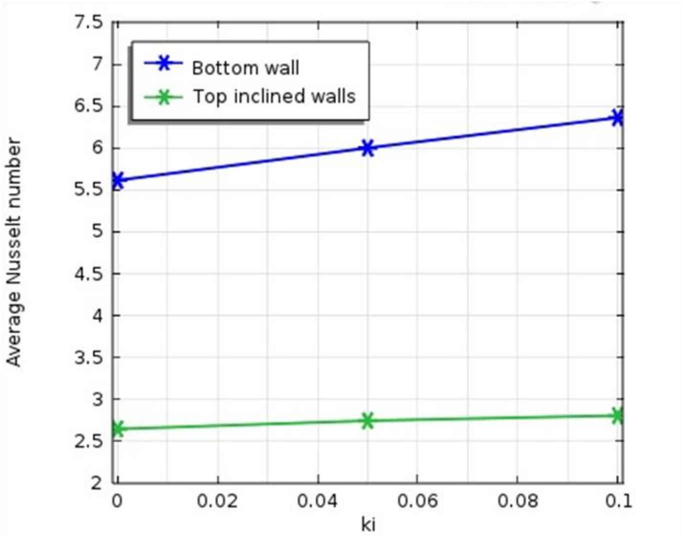

Fig.6. Effect of χ on heat transfer

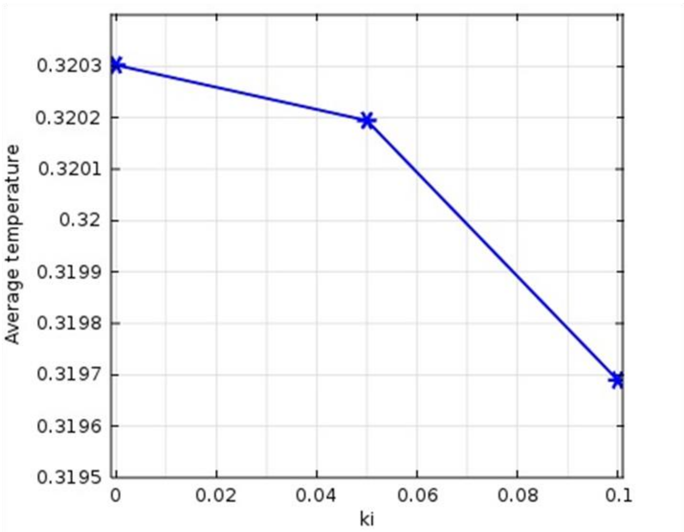

Fig.7. Effect of χ on average temperature

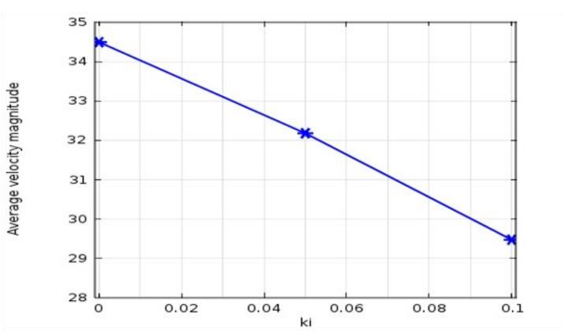

Fig.8. Effect of χ on average

4.5 Average temperature and average velocity

Fig. 7 demonstrates the distribution of average temperature with the nanofluid volume fraction. It is seen that the average temperature decreases for increasing values of χ. The average velocity in the domain is depicted in Fig.8 which is also decreased by the increment of χ. The movement of the fluid becomes slower due to higher values of χ.

5. CONCLUSION

The prime objective of the current investigation is to analyze a physical as well as computational insight due to heatflow for natural convection within a prismatic enclosure filled with nanofluid. The key controlling parameter for this analysis is which govern the overall heat transfer rate, i.e. Nusselt number. The heat transfer rates have analyzed with average Nusselt number for the top inclined walls and the bottom wall of the enclosure. The motivation is to understand the effect of the parameter on the heat flow process. The visualization of heat flow inside any cavity is incomplete unless we know about the heat flow and hence we have introduced the heatline concept in the prismatic enclosure which enables us to understand the heat flow trajectory. During conduction dominant heat transfer, it is observed that isotherms, streamlines and heatlines are found to be smooth. Also, the heatlines are seen normal to the isotherm during the heat transfer. However, as χ increases, convection is weaken. But heat transfer is increased due to conduction.

6. ACKOWLEDGEMENT

The present work is done in the department of mathematics BUET.

7. REFERENCES

[1] T. Basak, G. Arvind and S. Roy, Visualization of heat flow due to natural convection within triangular cavities using Bejan's heatline concept, *Int. J. Heat Mass Transfer*, vol. 52 (11-12), pp. 2824-2833, 2009.

[2] T. Basak, S. Roy, D. Ramakrishna and I. Pop, Visualization of Heat Transport during Natural Convection Within Porous Triangular Cavities via Heatline Approach, *Numerical Heat Transfer, Part A*, vol. 57 (6), pp. 431-452, 2010.

[3] T. Basak, S. Roy and I. Pop, Heat flow analysis for natural convection within trapezoidal enclosures based on heatline concept, *Int. J. Heat Mass Transfer*, vol. 52 (11-12), pp. 2471–2483, 2009.

[4] R. Anandalakshmi and T. Basak, Heatline based thermal management for natural convection in porous rhombic enclosures with isothermal hot side or bottom wall, *Energy Conversion and Management*, vol. 67, pp. 287–296, 2013.

[5] T. Basak, S. Roy and I. Pop, Heat flow analysis for natural convection within trapezoidal enclosures based on heatline concept, *Int. J. Heat Mass Transfer*, vol. 52, pp. 2471–2483, 2009.

[6] S. Kimura and A. Bejan, The heatline visualization of convective heat-transfer, *ASME J. Heat Transfer*, vol. 105 (4), pp. 916–919, 1983.

[7] Bejan, Convection Heat Transfer, third ed., Wiley, Hoboken, NJU, 1984.

[8] F.L. Bello-Ochende, A heat function formulation for thermal convection in a square cavity, *Int. Commun. Heat Mass Transfer*, vol. 15, pp. 193–202, 1988.

[9] V.A.F. Costa, Heatline and massline visualization of laminar natural convection boundary layers near a vertical wall, *Int. J. Heat Mass Transfer*, vol. 43 (20), pp. 3765–3774, 2000.
[10] V.A.F. Costa, Unified streamline, heatline and massline methods for the visualization of two-dimensional heat and mass transfer in anisotropic media, *Int. J. Heat Mass Transfer*, vol. 46 (8), pp. 1309–1320, 2003.
[11] V.A.F. Costa, Bejan's heatlines and masslines for convection visualization and analysis, *Appl. Mech. Rev.*, vol. 59 (3), pp. 126–145, 2006.
[12] Mukhopadhyay, X. Qin, S.K. Aggarwal and I.K. Puri, On extension of heatline and massline concepts to reacting flows through use of conserved scalars, *ASME J. Heat Transfer*, vol. 124 (4), pp. 791–799, 2002.
[13] Mukhopadhyay, X. Qin, S.K. Aggarwal and I.K. Puri, Visualization of scalar transport in non-reacting and reacting jets through a unified ‘‘heatline" and ‘‘massline" formulation, *Numer. Heat Transfer, Part A*, vol. 44 (7), pp. 683–704, 2003.
[14] Q.H. Deng and G.F. Tang, Numerical visualization of mass and heat transport for conjugate natural convection/heat conduction by streamline and heatline, *Int. J. Heat Mass Transfer*, vol. 45 (11), pp. 2373–2385, 2002.
[15] Dalal and M.K. Das, Heatline method for the visualization of natural convection in a complicated cavity, *Int. J. Heat Mass Transfer*, vol. 51 (1-2), pp. 263-272, 2008.
[16] S. J. Yaseen, Numerical study of steady natural convection flow in a prismatic enclosure with strip heater on bottom wall using FLEXPDE, *Diyala Journal of Engineering Sciences*, vol. 7 (1), pp. 61-80, 2014.
[17] K. F. U. Ahmed, S. Parvin and Ali J. Chamkha, Numerical analysis based on heatline approach for natural convection flows within prismatic enclosures, International Journal of Energy & Technology Vol. 7 (2), pp. 19-29, 2015
[18] S. Parvin, K.F.U. Ahmed, M.A. Alim and N.F. Hossain , Heat transfer enhancement by nanofluid in a cavity containing a heated obstacle, International Journal of Mechanical and Materials Engineering (IJMME), 7 (2) pp. 128-135, 2012.
[19] Rehena Nasrin, Salma Parvin, Investigation of buoyancy-driven flow and heat transfer in a trapezoidal cavity filled with water–Cu nanofluid, International Communications in Heat and Mass Transfer 39 (1) pp. 270–274, 2012.
[20] E. Abu-Nada and A. J. Chamkha, Effect of nanofluid variable properties on natural convection in enclosures filled with a CuO-EG-Water nanofluid, Int. J. Therm. Sci. 49 pp. 2339-2352, 2010.
[21] Salma Parvin and A.J. Chamkha, An Analysis on Free Convection Flow, Heat Transfer and Entropy Generation in an Odd-shaped Cavity filled with Nanofluid, International Communications in Heat and Mass Transfer 54 pp. 8–17, 2014.
[22] S. Teja, M. P. Beck, Y. Yuan and P. Warrier, The limiting behavior of the thermal conductivity of nanoparticles and nanofluids, J. Applied Physics, 107 pp. 114319, 2010.
[23] Salma Parvin, M.A. Alim, N.F. Hossain, Prandtl number effect on cooling performance of a heated cylinder in an enclosure filled with nanofluid, International Communications in Heat and Mass Tran. 39, pp. 1220–1225, 2012.
[24] J.N. Reddy and D.K. Gartling, The finite element method in heat transfer and fluid dynamics, CRC Press, Inc., Boca Raton, Florida, 1994.

8. NOMENCLATURE

Symbol	Meaning	Unit
g	acceleration due to gravity	[ms^{-2}]
k	thermal conductivity	[$Wm^{-1}K^{-1}$]
L	length of the base and height of the prismatic cavity	[m]
Nu	Nusselt number	
p	dimensional pressure	[Nm^{-2}]
P	dimensionless pressure	
Pr	Prandtl number	
Ra	Rayleigh number	
T	temperature	[K]
u, v	velocity components	[ms^{-1}]
U, V	dimensionless velocity components	
x, y	distance along x- and y-coordinates	[m]
X, Y	dimensionless distance along x- and y- coordinates	
	Greek symbols	
ν	kinematic viscosity of the fluid	[m^2s^{-1}]
θ	dimensionless temperature	